Front. Electr. Electron. Eng. China 2008, 3(1): 90–95
DOI 10.1007/s11460-008-0023-5

RESEARCH ARTICLE

Liye LIU, Yi SU, Junjie MAO

FDTD analysis of ground-penetrating radar antennas with shields and absorbers

Abstract One of the most critical hardware components of a ground-penetrating radar (GPR) is the antenna system. Important parameters of antennas, such as antenna bandwidth, radiation waveform and cross coupling determine the GPR system performance. The modified TEM horn antenna with distributed resistor load is presented in this paper, and the radiation properties of the antenna with the shields and absorbers are studied through the three-dimensional finite-difference time-domain (FDTD) scheme. Simulations show that the direct signal coupled from the transmitter is decreased by means of the shields and absorbers. Therefore, using the antenna in the GPR system can improve the signal-to-clutter ratio and the dynamic range of the system.

Keywords ground-penetrating radar (GPR), antenna, finite-difference time-domain (FDTD), generalized perfectly matched layer (GPML)

1 Introduction

The ground-penetrating radar (GPR) system using baseband pulses is greatly expected to be an effective tool for nondestructively sensing subsurface environment. Various GPR systems are employed to detect buried objects such as pipes, cables, mines and unexploded ordnance (UXO) under the surface of the earth [1].

The system detects and images the buried object through the transmitting and receiving antenna with broad bandwidth, good efficiency and low antenna clutter. The antenna system is one of the most critical hardware components of the GPR system. Its performance determines the distinguishing capability, locating and target recognition of the system. The antenna is covered with a conducting cavity to prevent electromagnetic radiation from affecting other electric systems as well as block the antenna from receiving undesired signals from the air. The wave absorber is attached to the inner walls of the conducting cavity to reduce the multiple reflections in the cavity.

The advancement of the finite-difference time-domain (FDTD) simulation technique has made it possible to accurately evaluate some complex and loaded antennas used in the GPR system. The antenna radiation characteristic, particularly in time and frequency domains, and electromagnetic radiation action can be derived through FDTD simulation, of which the results can help optimize the antenna properties [2,3]. In this paper, the FDTD scheme is used to analyze the antenna system model, including the GPR antenna, shields and absorber. Finally, the influence of shields and absorbers on antenna radiation properties and the scattering signal of buried objects are studied.

2 FDTD model of the resistive-loaded GPR antenna

2.1 The antenna model

GPR systems usually use ultra-wide band electromagnetic pulse. It demands that the antenna have broadband input impedance characteristics and fewer multiple reflections of the input signal from different parts of the antenna. There are only a few types of antennas that are widely utilized in GPR systems, such as resistively loaded cylindrical monopoles, resistively or resistor-loaded bow-tie antennas, spiral antennas, and TEM horns and their modifications [4–11]. The bow-tie antenna, covered with a conducting cavity which connects the shield with resistors to control the oscillation of the signal, has been analyzed in Refs. [4,5]. The capacity-tapered bow-tie antenna was described in

Translated from *Chinese Journal of Radio Science*, 2006, 21(3): 422–427 [译自: 电波科学学报]

Liye LIU (✉), Yi SU, Junjie MAO
College of Electronic Science and Engineering, National University of Defense Technology, Changsha 410073, China
E-mail: liu_liye@tom.com

Ref. [8], and it was proven that the amplitude and the shape of the transmitting waveforms can be optimized by using this kind of antenna. But it is relatively difficult to theoretically simulate and optimize various antenna parameters due to the complexity of the antenna geometry. Lee [9] shows three different resistance profiles of the resistive cards (*R*-cards) which are used to optimize the radiated field of the antenna. But the manufacturing of the continuous resistive *R*-cards is difficult to realize in practice. In this paper, we present a novel GPR antenna where the dipole with discrete exponential resistive is above the image plane. This antenna can terminate the ringing, and is easier to manufacture than the continuous resistive loading antenna [11].

Figure 1(a) shows the geometry of the GPR antenna with discrete resistor load. Figures 1(b) and (c) demonstrate the frontal and side elevation of the antenna with shields and absorbers. The tapered monopole and the perfect electrical conductors (PEC) image make up the GPR antenna. The monopole rests above the image plane, and consists of multi-slots with loaded resistors. The resistive value increases exponentially from the position x_0 (the starting position of resistive loading along the monopole) to the open end. The resistor profiles are expressed as:

$$R = R_{\min} \exp\left\{\gamma \frac{x - x_0}{l}\right\}, \tag{1}$$

where $R_{\min}$ is the resistor value of the starting position, γ is the optional coefficient, x is the position along the resistive monopole, l is the total length of the monopole.

There is a lumped circuit element that is small enough to be contained in one FDTD cell. According to Ref. [3], the finite difference equation for the electric field components can be modified as (here, we only present the formulation of E_z component, the formulation of E_x and E_y component. The equations about magnetic field component are not modified.):

$$E_z^{n+1}\left(i,j,k+\frac{1}{2}\right) = \frac{C}{C+G\Delta t} E_z^n\left(i,j,k+\frac{1}{2}\right) + \frac{\Delta x \Delta y \Delta t}{C\Delta z + G\Delta z \Delta t}\left(\nabla \times \mathrm{H}^{n+1/2}\right)_z, \tag{2}$$

where $C = \varepsilon \Delta x \Delta y / \Delta z$ is the lumped "parallel plate" capacitance of the cell, and $G = \sigma \Delta x \Delta y / \Delta z = 1/R$ is the lumped conductance of the cell parallel with the capacitance. Thus, a lumped load that is a parallel combination of a capacitor and a conductance (resistance) can be simply modeled by setting the cell values of ε and σ appropriately.

2.2 Model for feed region

The conversion scheme introduced in Ref. [12] is adopted in this paper. The voltage and current component model is employed in the coaxial transmission line, and the field components of the connection between the coaxial line and the Yee grid are depicted as:

$$\begin{aligned} H_z^{n+\frac{1}{2}}&\left(i_a+\frac{1}{2}, j_a+\frac{1}{2}, k_a\right) \\ &= H_z^{n-\frac{1}{2}}\left(i_a+\frac{1}{2}, j_a+\frac{1}{2}, k_a\right) + \frac{\Delta t}{\mu_0 \Delta y}\left[E_x^n\left(i_a+\frac{1}{2}, j_a+1, k_a\right)\right. \\ &\quad \left. - \frac{2}{\Delta x \ln(\Delta x/a)} V^n(j_a)\right] - \frac{2\Delta t}{\mu_0 \Delta x \ln(\Delta x/a)} \\ &\quad \times E_y^n\left(i_a+1, j_a+\frac{1}{2}, k_a\right), \end{aligned} \tag{3}$$

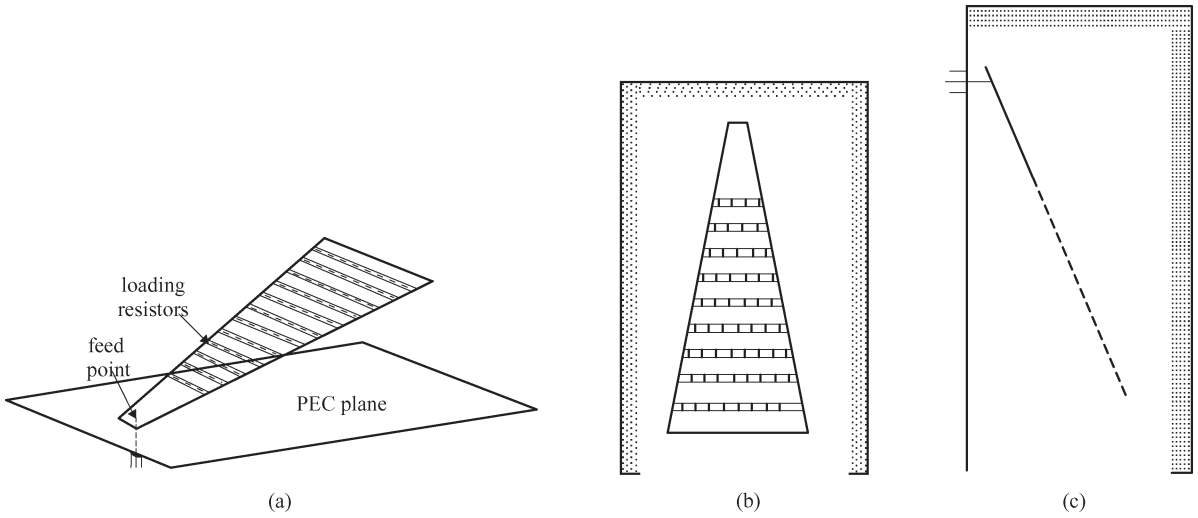

Fig. 1 Geometry of the GPR antenna with shields and absorbers. (a) The GPR antenna with discrete resisting load; (b) elevation; (c) side elevation

$$I^{n+\frac{1}{2}}\left(j_t+\frac{1}{2}\right)=\Delta z\left[H_x^{n+\frac{1}{2}}\left(i_a, j_a+\frac{1}{2}, k_a+\frac{1}{2}\right)-H_x^{n+\frac{1}{2}}\left(i_a, j_a+\frac{1}{2}, k_a-\frac{1}{2}\right)\right]-\Delta x\left[H_z^{n+\frac{1}{2}}\left(i_a+\frac{1}{2}, j_a+\frac{1}{2}, k_a\right)-H_z^{n+\frac{1}{2}}\left(i_a-\frac{1}{2}, j_a+\frac{1}{2}, k_a\right)\right], \quad (4)$$

where, a is the radius of the coaxial transmission line.

The coupled field components of feed point are introduced through Eqs. (3) and (4), of which the former indicates the relation between the voltage component and the magnetic component, while the latter demonstrates the relation between the magnetic and the current components.

2.3 The equivalent model of absorbers

In the transmitter-receiver configuration, the receiving antenna collects not only the fields scattered from the target (S), but also the direct signal coupled from the transmitter (D) as well as the signal reflected from the ground (G). When D, G and S signals are superposed at the receiver location to compose a general signal $D+G+S$, the energy of the S signal constitutes a very small portion of the total received energy. However, the main problem encountered in the bistatic GPR system is that the D signal is too large with respect to the desired S signal. Therefore, it is quite difficult to detect the scattered signal in the total received signal. Though the direct wave can be removed by various signal process methods, the dynamic range of the system is not essentially enhanced.

In this paper, in order to overcome this difficulty, the transmitting and the receiving antennas are isolated by conducting walls. The shield walls enclose the two antennas in two chambers, leaving only the bottom faces of the chambers open, as displayed in Fig. 1. Making use of bare conducting walls yields large and slow-decaying oscillations due to the resonance effects. In practice, these resonance effects are prevented by mounting high-frequency absorbers on the inner side of the shield walls. However, FDTD simulations of such novel materials entail enormous computation though these high-performance absorbers maintain rapidly decaying electromagnetic fields in small thickness. Therefore, the inner faces of the conducting shield wall are coated with three-cell-thickness perfectly matched layer (PML) absorber which is described in Ref. [13].

2.4 Absorbing boundary conditions

To simulate the computational domain extended to infinity, the absorbing boundary condition (ABC) is utilized. Generally, in the application of the ground penetrating radar antennas, the soil is modeled as a homogeneous lossy medium. Therefore, although Berenger's perfectly matched layer (PML) ABC [14] is very effective in absorbing propagating waves in lossless media, it exerts little influence on absorbing evanescent waves. In consequence, the generalized perfectly matched layer (GPML) ABC [15] achieves near-perfect absorption of propagating and evanescent waves of any frequency and any angle of incidence in both lossless and lossy media. The thickness of the GPML is taken as five cells in this paper.

3 Simulation results

3.1 The effect of the shield and absorbers

The geometry of the antenna is shown as Fig. 1. The PEC plane is 30 × 24 cm^2; the length of the monopole is 20 cm; the angle between the monopole and the PEC plane is 20°; the number of resistive strip is 15; the distance between slots is 1 cm; $R_{\min}=2.5\ \Omega$, $x_0=4$ cm and $\gamma=8$. The computational domain is divided into 0.5 cm cubic cells. The E- and H-field components at each cell are calculated from the finite-difference expressions based on Yee's algorithm. The input signal to the antenna is a differentiated Gaussian pulse of the following form:

$$v(t)=v_0\frac{(t-t_0)}{\tau}\exp\left\{-\frac{(t-t_0)^2}{\tau^2}\right\}, \quad (5)$$

where $v_0=2.5$ V, $t_0=0.667$ ns and $\tau=t_0/4$.

Figure 2 shows the FDTD-calculated transmitting waveform of the antenna under three conditions: without shield, with shield and with shield and absorbers. The position of observation is set below the feed point at a depth of 40 cm. The size of the cavity is 30 cm × 24 cm × 20 cm. The amplitude of radiation waveform increases when the antenna is coated by the conducting cavity, but the ringing is raised due to the multiple reflections between the antenna and the cavity. The ringing makes the detection of the scattering signal of the buried object difficult or even impossible. The wave absorber is attached to the inner walls of the conducting cavity to reduce the multiple reflections in the cavity.

Figure 3 shows the near-zone amplitude radiation patterns for the component of the electric field E_y when the antenna is without/with shield and absorbers. The radial distance between the feed point and the observed point is set to 50 cm. From the simulation results, it can be seen that the coated antenna pattern in H-plane is narrower than the uncoated antennas, and the pattern in E-plane is almost unmovable. Consequently, the D signal may decrease and the signal-to-clutter ratio of the system is improved.

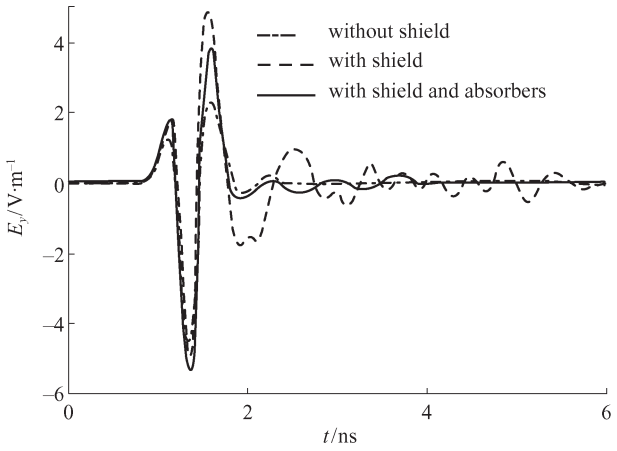

Fig. 2 Comparison of the transmitted waveforms of the antenna

3.2 The scattering signal of buried objects

One of the most important properties of the transmitting antenna is the size of the illuminated spot on the air-ground interface and the spatial distribution of the maximum value of the radiated signal in the near field during the entire observation time (footprint). The GPR antenna should produce an optimal footprint on the ground surface and under it (the size of the footprint should be sufficiently large for synthetic aperture radar (SAR) processing while at the same time it should be small enough to reduce surface clutter). The footprint intersection between the transmitting and receiving antennas may influence the scattering signal of the buried objects.

Figure 4 shows the received signal by the receiving antenna and the corresponding scattering signal of layer mediums when transmitting and receiving antennas are without/with shield and absorbers. It is assumed that the layer medium is lossy and homogeneous with the perfectly smooth surface. The parameters of the upper medium are as follows: $\varepsilon_r = 4.0$, $\sigma = 0.005$ S/m and the layer thickness is 20 cm. The parameter of the second medium are: $\varepsilon_r = 8.0$ and $\sigma = 0.02$ S/m. The antennas' height above the ground is 20 cm, and the space between the two feed points is 25 cm. Figure 5 shows the received signal and the corresponding scattering signal of buried conducting strip. The earth is modeled as a homogeneous lossy medium ($\varepsilon_r = 4.0$, $\sigma = 0.02$ S/m), and the ground is a perfectly smooth surface. The size of the strip is

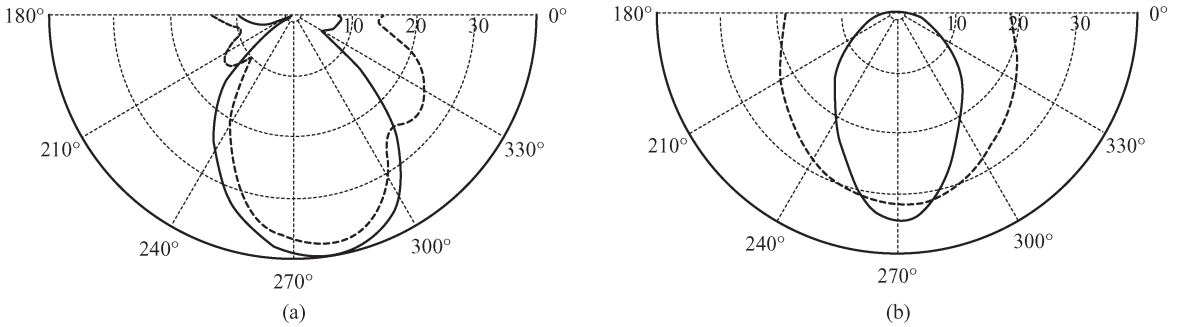

Fig. 3 Near-field patterns of E_y in E-plane (Y-Z plane) and H-plane (X-Z plane). (a) E-plane; (b) H-plane (-----without shield, —with shields and absorbers)

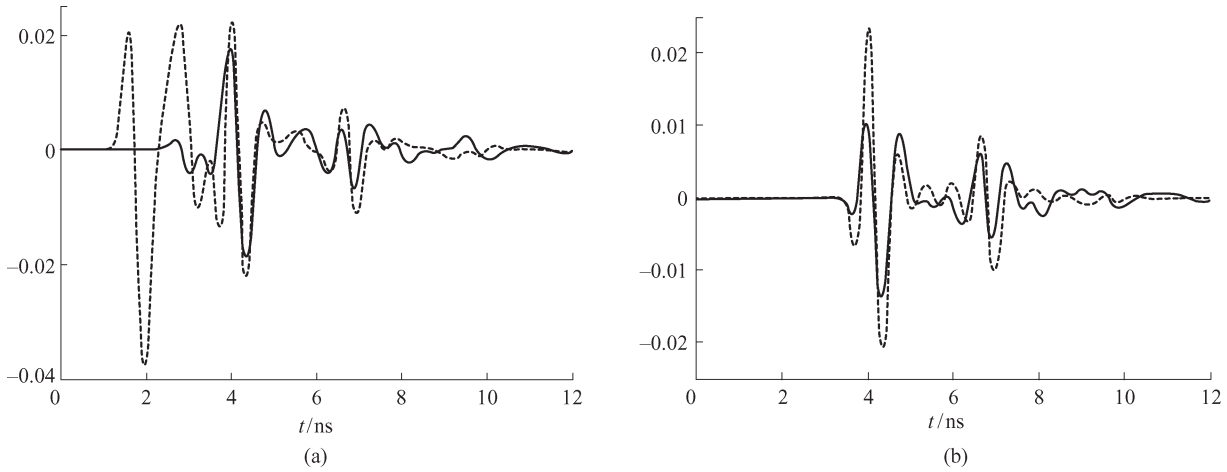

Fig. 4 Comparison of the scattering signal of layer mediums. (a) Received signal; (b) scattering signal of layer mediums (-----without shield, ——with shields and absorbers)

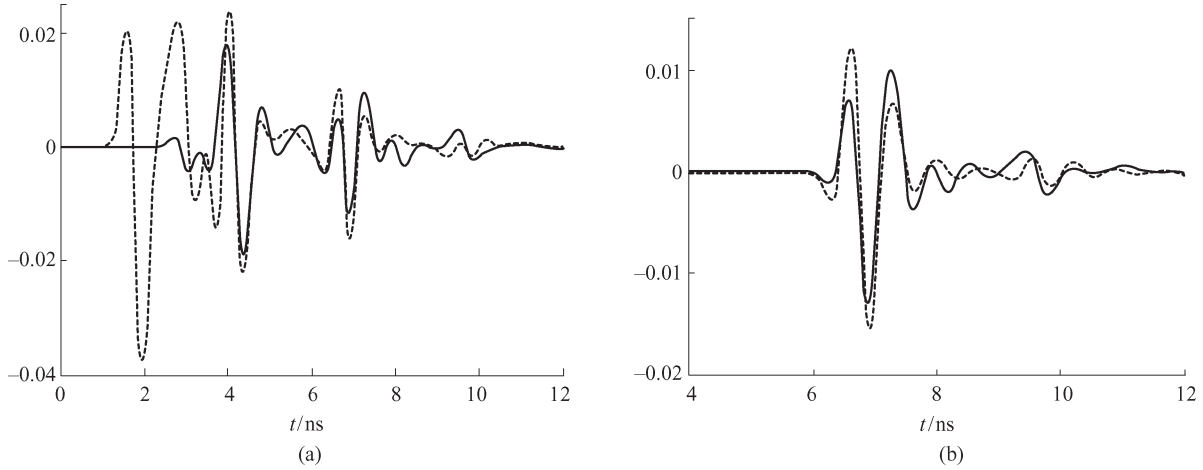

Fig. 5 Comparison of the scattering signal of buried objects. (a) Received signal; (b) scattering signal of buried conducting strip (-----without shield, —with shields and absorbers)

10×30 cm^2, and it is symmetrically buried below the two antennas at a depth of 40 cm.

Simulation results indicate that the buried objects and layer mediums may be detected through the modified TEM horn antenna with resistive loading. By means of the shield and absorbers, the direct signal coupled from the transmitter is suppressed. The scattering signal is decreased slightly because the footprint intersection of the antennas diminishes. Figure 4 shows that the ratio of the direct coupling signal (D), the ground reflection signal of the upper layer (G_1) and the reflection signal of the second layer (G_2) is $D{:}G_1{:}G_2 = 1{:}0.727{:}0.316$ when uncoated antennas are used, and the ratio becomes $D{:}G_1{:}G_2 = 1{:}1.383{:}0.679$ when using antennas with shields and absorbers. It is shown in Fig. 5 that the ratio of the direct wave to the object signal is 2.23 using uncoated antennas, and it becomes 1.61 when using the coated antennas. Therefore, by means of attaching the wave absorber to the inner walls of the conducting cavity, the signal-to-clutter ratio and dynamic range of the GPR system may be enhanced. And the method helps detect the buried objects and bounded layered medium.

4 Conclusions

The modified TEM horn antenna, with discrete exponential resistive load shown in Fig. 1, is presented in this paper. The radiation properties of the antenna with shield and absorbers have been studied extensively through the FDTD method, and the comparison of the results of the scattering signal of buried objects are demonstrated. The antenna is covered with a conducting cavity to prevent electromagnetic radiation from affecting other electric systems, and also to prevent the antenna from receiving undesired signals arrived from the air. By means of attaching the wave absorber to the inner walls of the conducting cavity, the multiple reflections between the antenna and the cavity are reduced. The dynamic range of the GPR system may be enhanced by using the antenna with shield and absorbers.

Acknowledgements This work was supported by the National Basic Research Program of China (No. 2001AA132020).

References

1. Daniels D J, Gunton D J, Scott H F. Introduction to subsurface radar. In: Proceedings of IEE, 1988, 135(4): 278–320
2. Ge D B, Yan Y B. The finite difference time domain method for electromagnetic wave. Xi'an: Xidian University Press, 2002 (in Chinese)
3. Kunz K S, Luebbers R J. The finite difference time domain method for electromagnetic. Boca Raton: CRC Press, 1993
4. Bourgeois J M, Smith G S. A fully three-dimensional simulation of a ground-penetrating radar: FDTD theory compared with experiment. IEEE Transactions on Geoscience and Remote Sensing, 1996, 34(1): 36–44
5. Zhan Y, Liang C H, Fang G Y, et al. Simulation of bow-tie antennas above ground and its applications, Chinese Journal of Radio Science, 2000, 15(2): 134–138 (in Chinese)
6. Yan X R, Jin Y S, Luo C M. Analysis of wide-band properties and efficiency for dipole antennas with resistive and capacitive loadings. Chinese Journal of Radio Science, 2000, 15(2): 169–173 (in Chinese)
7. Zhou W H, He J G, Zhou D M. Optimized design of a new kind of GPR planar antenna. Chinese Journal of Radio Science, 2004, 19(3): 371–373 (in Chinese)
8. Lestari A A, Yarovoy A G, Ligthart L P. Improvement of bow-tie antennas for pulse radiation. IEEE Antennas and Propagation Society International Symposium, 2002, 4: 566–569
9. Lee K-H, Venkatarayalu N V, Chen C-C. Numerical modeling development for characterizing complex GPR problems. SPIE, 2002, 4758: 652–656
10. Lacko P R, Franck C C, Johnson M, et al. Archimedean-spiral and log-spiral antenna comparison. SPIE, 2002, 4742: 230–236
11. Liu L Y, Su Y, Liu K K, et al. Radiation characteristics of GPR antenna through FDTD method, Journal of Microwave, 2005, 21: 91–95 (in Chinese)

12. Maloney J G, Shlager K L, Smith G S. A simple FDTD model for transient excitation of antennas by transmission lines. IEEE Transactions on Antennas and Propagation, 1994, 42(2): 289–292
13. Gürel Levent, Oğuz U. Simulations of ground-penetrating radars over lossy and heterogeneous grounds. IEEE Transactions on Geoscience and Remote Sensing, 2001, 39(6): 1190–1197
14. Berenger J P. A perfectly matched layer for the absorption of electromagnetic waves. Journal of Computational Physics, 1994, 114(2): 185–200
15. Fang J Y, Wu Z H. Generalized perfectly matched layer for the absorption of propagating and evanescent waves in lossless and lossy media. IEEE Transactions on Microwave Theory Techniques, 1996, 44(12): 2216–2222